A limitation of two-state analysis for transitions between disordered and weakly ordered states

Dudley H Williams, Ben Bardsley, Wakako Tsuzuki* and Alison J Maguire†

Background: The stability of the secondary structure of particular peptide regions is often used to investigate the involvement of the region in protein folding. When analysing the relatively small populations of associated states that are formed by weak interactions (i.e. those interactions that are comparable to thermal energies), it is common practice to characterise the associated state by a parameter that is measured when this state is highly occupied. The accuracy of this method, however, has not yet been determined.

Results: Using as a model the vancomycin group of antibiotics, either forming dimers or binding to cell wall precursors, we have investigated the dependence of the limiting (i.e. fully associated) chemical shifts of two protons on the equilibrium constants for the formation of the fully associated states. The chemical shift shows a large variation with the equilibrium constant for the formation of the fully associated state.

Conclusions: The results demonstrate, in two systems, that a parameter representing a fully associated state (chemical shift) varies greatly with the equilibrium constant for the formation of that associated state. The results have implications for two-state analyses of populations of protein fragments in which a parameter representing the fully associated state is taken to be independent of the equilibrium constant for its formation. Using two-state analysis to determine the population of associated states of protein fragments could result in an underestimation of the population of these associated states.

Address: Cambridge Centre for Molecular Recognition, Department of Chemistry, Lensfield Road, Cambridge CB2 1EW, UK.

Present addresses: *National Food Research Institute, Ministry of Agriculture, Forestry and Fisheries, 2-1-2 Kannondai, Tsukuba, Ibaraki, 305, Japan. †Public Health and Clinical Microbiology Laboratory, Level 6, Addenbrookes Hospital, Hills Road, Cambridge, CB2 2QW, UK.

Correspondence: DH Williams
E-mail: dhw1@cus.cam.ac.uk

Key words: dimerisation, ensemble of states, glycopeptide antibiotics, protein fragment population, two-state analysis

Received: **23 May 1997**
Accepted: **13 June 1997**

Chemistry & Biology July 1997, 4:507–512
http://biomednet.com/elecref/1074552100400507

Introduction

In the analysis of a reaction:

$$A + B \rightarrow A.B \quad (1)$$

in which A and B are joined by a bond that is strong compared to thermal energies, the relative populations of the species involved can be reliably derived by a two-state (reactant/product) analysis. Similarly, for a unimolecular change:

$$A \rightarrow A' \quad (2)$$

in which the reorganisation of the bonding on passing from A to A′ involves bonds that are strong compared to thermal energies, a two-state analysis can also be applied. In these cases, if a parameter can be measured, that is characteristic of 100% population of the species on the right hand side (RHS) of the equation (x_{prod}), (whereas this parameter has a value of x_{react} for the species on the left hand side), and if, under conditions where both species are populated, an experimental value of the parameter is x_{exp}, then:

$$\text{Fractional population of species on the RHS} = \frac{x_{exp} - x_{react}}{x_{prod} - x_{react}} \quad (3)$$

A dilemma arises, however, when the bonds made or broken have strengths that are comparable to thermal energies. As conditions are altered so as to vary the populations of the species involved, there is no guarantee that x_{prod} is a constant. Nevertheless, it is still common practice to apply Equation 3 and the analysis then becomes known as a two-state analysis. The reason that Equation 3 may be inapplicable in these cases can be seen by comparing a potential energy well (using a diatomic analogy) for a strongly bound species (Figure 1a) with that of a weakly bound species (Figure 1b) [1,2]. In the former case, as a variable is changed to decrease the population of a bound state (e.g. the temperature is increased), the structure of the bound state is not changed significantly because higher vibrational levels of this state do not become sufficiently occupied to change the internuclear distance that is used to describe it. In the case of a shallow well (Figure 1b), however, higher vibrational (and rotational) levels are accessible at the higher temperatures because these levels are very closely spaced near the mouth of the well. It is therefore expected that the average bond length in this state may increase significantly; the structure is not constant. The postulated effect is analogous to the expression of heat capacity in a solid in which molecules are induced, by an increase in temperature, to increase their motions within their local

Figure 1

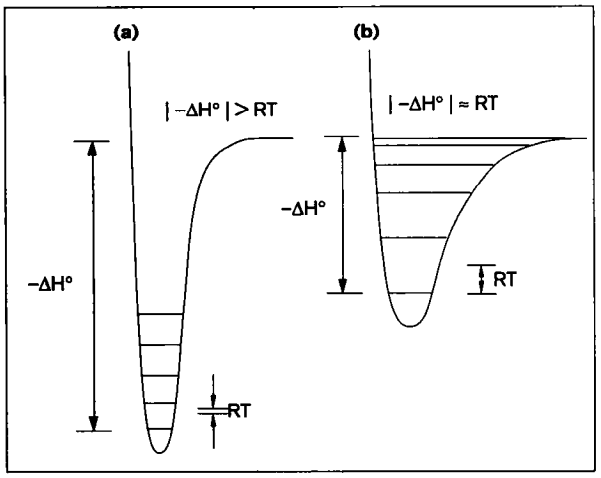

The potential energy wells for the dissociation, or disordering, of a bound state in which the energy required is **(a)** large compared to thermal energies and **(b)** small compared to thermal energies. ΔH°, change in enthalpy; R, the gas constant; T, temperature.

energy wells and thereby induced to undergo a decrease in their local bonding (requiring heat uptake). By analogous reasoning, if, in the case of Figure 1b, the well is made even more shallow relative to vibrational and rotational energies (e.g. by changing the solvent for a peptide with limited propensity to form an α helix from trifluoroethanol (TFE) to water), then the average bond lengths of the weak bonds in the helix might reasonably be expected to increase. So, as the free energy for helix formation is made less negative, the structure of the helix should change and become looser. The parameter (x_{prod}) describing such a looser state might thereby reasonably be expected to become smaller (relative to x_{react}) than for the tighter structure.

As far as we are aware, clear experimental evidence for the above proposed effect, in which the free energy changes for systems involving weak interactions can be systematically changed and measured, has not been described for complex systems of biological interest. Indeed, in the case of a unimolecular change (Equation 2) and where the parameters of interest are time-averaged, there seems to be no way to test the hypothesis. The very act of modifying the experiment to bring the ordered

Figure 2

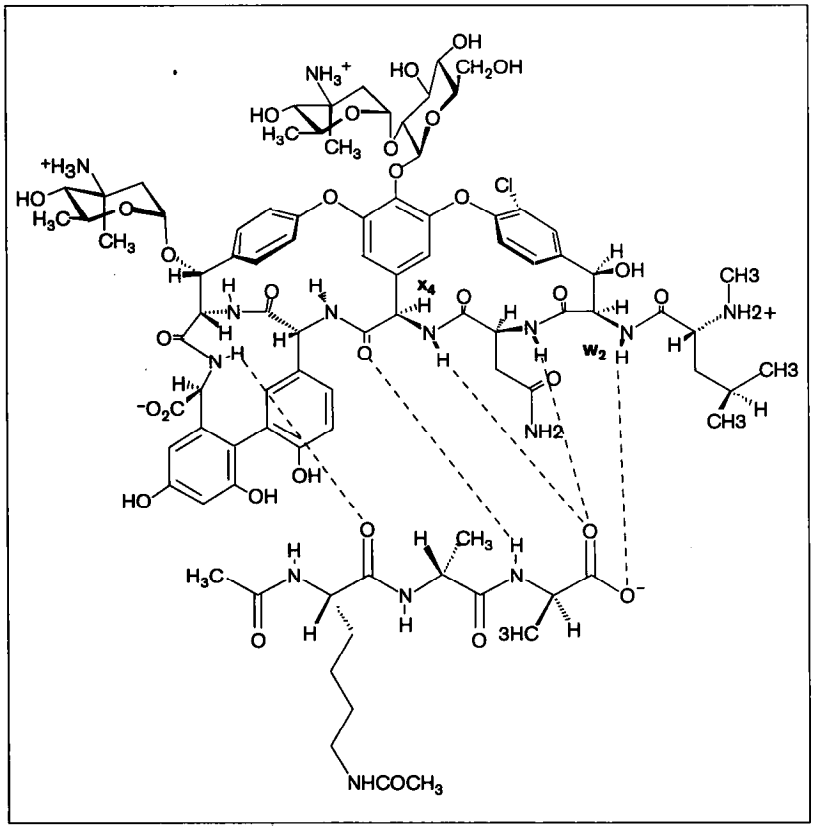

An exploded view of the complex of the antibiotic eremomycin with di-*N*-Ac-Lys–D-Ala–D-Ala. The monitored protons w_2, in the carboxylate binding pocket of the antibiotic, and x_4, which lies in the dimer interface, are indicated.

Figure 3

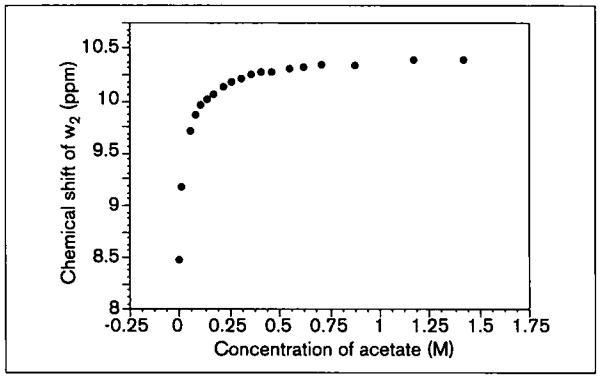

Determination of the limiting chemical shift for the antibiotic proton w_2. A plot of the chemical shift of w_2 of eremomycin against the concentration of added acetate.

Figure 4

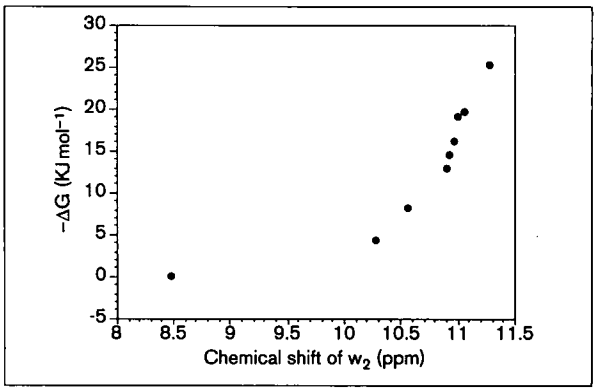

A plot of ligand-binding energy (ΔG) against the limiting chemical shift of the antibiotic proton w_2 for eremomycin, in complexes formed with various truncated bacterial cell-wall precursor analogues. In order of increasing magnitude of ΔG, the points represent the binding of the following ligands: none, acetate, di-*N*-Ac-Lys–D-Ala–D-lactate, *N*-Ac-Gly–Gly, *N*-Ac-D-Ala–Gly, *N*-Ac-D-Ala, *N*-Ac-Gly–D-Ala, *N*-Ac-D-Ala–D-Ala and di-*N*-Ac-Lys–D-Ala–D-Ala.

state nearer to the mouth of the potential well (Figure 1b) will simultaneously increase the population of the disordered state and so obscure the effect being investigated. In the case of a bimolecular association (Equation 1), however, a parameter that describes the fully bound state (x_{prod}) as it is brought nearer to the mouth of the potential well (where it might now be best described as an ensemble of canonical bound states) can still be obtained. This is because the concentration of one of the associating components can be increased such that, despite the smaller equilibrium constant for association, the second component becomes fully bound. Using this method (with a proton chemical shift of the fully bound state as the x_{prod} parameter), we have been able to show that x_{prod} does indeed undergo large variations as a function of the equilibrium constant K for Equation 1, in which the strengths of the bonds formed between A and B are comparable to thermal energies.

Results and discussion

In the formation of complexes of bacterial cell-wall precursor analogues (ligands) with glycopeptide antibiotics, the difference in chemical shift of an antibiotic proton (w_2, the amide proton of residue 2, which is involved in binding the carboxylate anion of the cell-wall peptide analogues, Figure 2) between the free and fully bound states can be measured [3,4]. This limiting chemical shift can be obtained by extrapolating the plot of chemical shift against concentration of ligand to infinite concentration of ligand (Figure 3). If the limiting chemical shifts of w_2 are plotted against the equilibrium constant for the antibiotic–ligand association, then a curve is obtained [3,4]. To illustrate this point, we show data for one antibiotic of the vancomycin group, eremomycin (Figure 4). A curve of this general shape is to be expected because, as the equilibrium constant for association of the ligand increases, the carboxylate/w_2 hydrogen bond will approach a limiting strength. The addition of further residues to the ligand, although providing extra binding energy, will therefore have a reduced effect on the chemical shift of w_2. In the present context, the point of importance is that the limiting downfield shift of w_2 increases dramatically with an increase in the equilibrium constant for the association [3,4]. For example, when binding to eremomycin, acetate has an association constant of ~10 M^{-1} compared to almost 10^5 M^{-1} for di-*N*-Ac-Lys–D-Ala–D-Ala; furthermore, the change in chemical shift of w_2 between the free and bound states for acetate is only ~65% of the shift change found for di-*N*-Ac-Lys–D-Ala–D-Ala. The much reduced downfield chemical shifts found for the fully bound states formed with smaller equilibrium constants are observed, despite the fact that the structural changes in the cell-wall analogues that lead to the reduced equilibrium constants are relatively remote from the monitored proton [3,4]. These observations are interpreted to mean that the complexes formed with small equilibrium constants are looser than those formed with large equilibrium constants, because the equilibrium length of the common weak bond formed at the carboxylate–antibiotic interface increases in the series di-*N*-Ac-Lys–D-Ala–D-Ala < *N*-Ac-D-Ala–D-Ala < *N*-Ac-D-Ala < acetate. We also infer that the extra interactions between the larger ligands (relative to acetate) and the antibiotic are instrumental in restricting the motion of the carboxylate anion in its binding site, thereby increasing its bonding affinity for the w_2 amide [1,3]. Clearly, x_{prod} decreases markedly as the equilibrium constant for the association decreases.

Figure 5

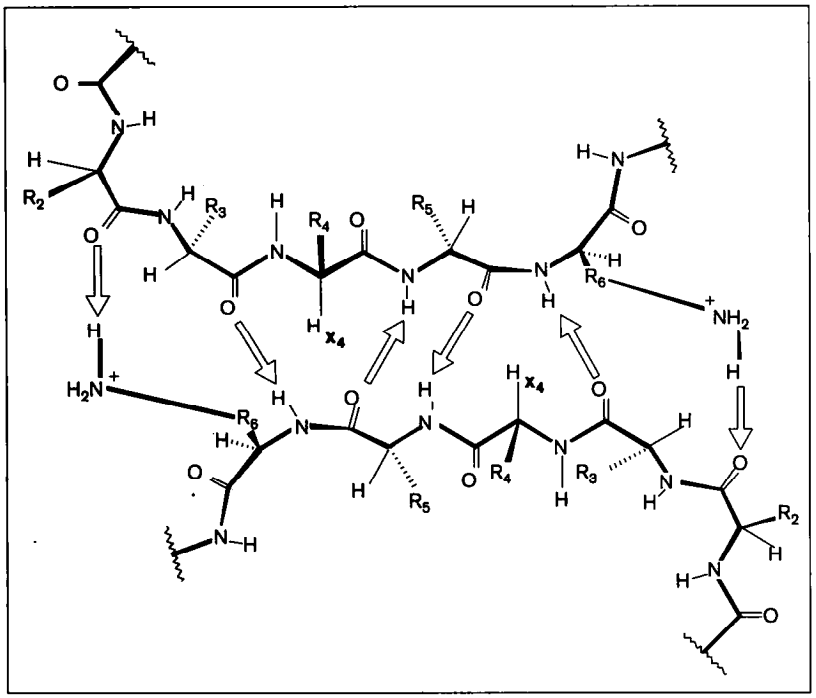

The hydrogen bonding network of the dimer formed between two molecules of eremomycin. The proton x_4 has a chemical shift that varies as a function of the dimerisation constant. The hydrogen bonds are indicated by the white arrows.

In order to investigate the generality of this phenomenon, we have also examined the dimerisation of a series of glycopeptide antibiotics (occurring through the formation of a number of amide–amide hydrogen bonds, Figure 5) [5].

Figure 6

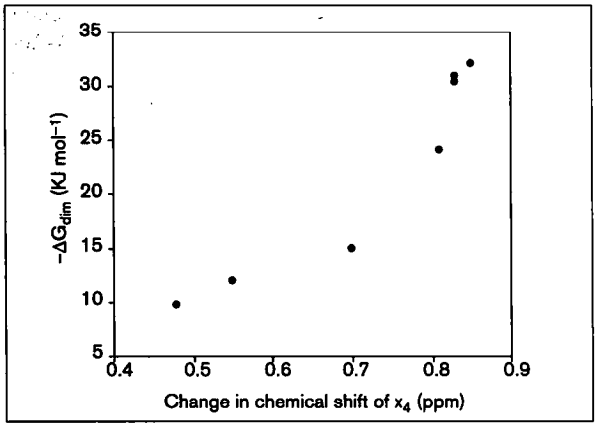

A plot of free energy of dimerisation against the change in chemical shift of the proton x_4 upon dimerisation for some glycopeptide antibiotics. In order of increasing magnitude of ΔG_{dim}, the points represent the dimerisation of the following antibiotics: ristocetin Y, monodechlorovancomycin, vancomycin, chloroeremomycin, eremomycin, biphenylchloroeremomycin and decaplanin.

In the present context, the advantages of this system are that upon dimerisation, a proton (x_4) located near the centre of the dimer interface undergoes a relatively large downfield shift [5], and that the limiting downfield shift of this proton can be determined for a series of antibiotics as the dimerisation constant varies from ~$10\,M^{-1}$ to $>10^5\,M^{-1}$. It is emphasised that the structural variables that cause this variation in dimerisation constant (e.g. the presence of certain sugars attached to amino acids 4 or 6 of the antibiotics) are all relatively remote from x_4 [6,7]. We observed that the downfield shift of x_4 upon dimerisation is, in the fully dimerised state, much smaller in those cases in which the equilibrium constant (K) for dimerisation is small (Figure 6). The chemical shift of x_4 upon dimerisation is likely to be significantly influenced by two factors. Firstly, it will be influenced by a reduction in the torsional motions of the dipoles of the amides that bond to each other at the dimer interface relative to their motions in the monomer [8,9]. This means that x_4 should, on average, be held nearer to the plane of the carbonyl group of residue 3 in the same half of the dimer, resulting in a downfield shift. Secondly, the chemical shift will be influenced by the proximity of x_4 to the carbonyl of residue 5 in the other half of the dimer, again resulting in a downfield shift [8,9]. We interpret the smaller limiting shift of x_4 at smaller equilibrium constants to mean that there is a reduced influence on its chemical shift from the carbonyl in the opposite half of the dimer and a reduced

Figure 7

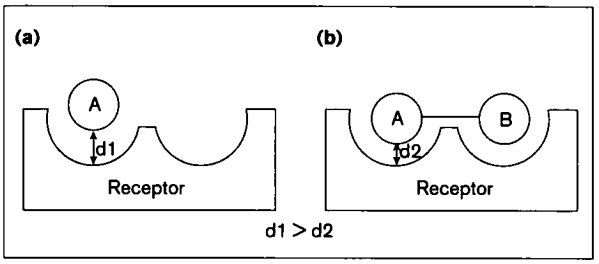

A schematic representation of **(a)** the association of an entity A with its receptor and **(b)** the association of the same entity A when attached via a strain-free linker to a second entity B that binds to a separate site on the same receptor. In (b), the association constant of the ligand with the receptor is high due to the cooperative enhancement to the binding of A provided by B. In this case, the complex formed is relatively tight and relatively few bound states are accessible to the ligand. As a result, the distance d2, the average distance between w_2 of a glycopeptide and the carboxyl group of the bound ligand, for example, (or, equally, between x_4 and the carbonyl group of the opposite half of a glycopeptide dimer) is relatively short. In (a), the association constant of the ligand with the receptor is low and a greater number of canonical bound states are accessible to the ligand as a result of the looser nature of the complex. The resultant average distance d1, which reflects the greater number of weakly bound states occupied by the complex, is therefore longer than d2. The distance d correlates directly with the parameter x_{prod} (e.g. a greater w_2/carboxyl hydrogen bond distance results in a smaller downfield chemical shift of w_2). At lower association constants, the larger number of occupied bound states therefore results in a lower value of x_{prod}.

rigidity of the peptide backbone as a result of longer equilibrium bond lengths across the dimer interface. The chemical shift changes parallel those observed for the system shown in Figure 2; x_{prod} decreases as the equilibrium constant for association decreases (Figure 6 compared to Figure 4). A schematic representation of this effect is shown in Figure 7.

It is clear from the above two sets of data (reflecting glycopeptide antibiotics binding to ligands and dimerisation of glycopeptide antibiotics) that unique bound states do not exist. By analogy, two-state analyses of β-sheet or α-helix formation from disordered states, via a number of conformationally averaged parameters (circular dichroism: molar ellipticity at 222 nm [10–16]; ^{1}H nuclear magnetic resonance (NMR) spectroscopy: $C^{\alpha}H$ chemical shifts [13,14,16–19], $^3J_{N\alpha}$ coupling constants [20], $d_{\alpha N}(i, i+1)$ vs. $d_{NN}(i, i+1)$ nuclear Overhauser effect (NOE) cross peak intensities [20,21]) may be subject to an error of similar origins. In such two-state analyses, it appears, by analogy to our results, that as K for the formation of the ordered state becomes smaller (e.g. K = 1 for unimolecular association), then x_{prod} for these conditions will be different from x_{prod} for the state as it exists in a protein from which the helical or hairpin fragment may have been derived. The reference values of x_{prod} used to calculate the populations of ordered structures of protein fragments at these low values of K may be inappropriate, having been measured under conditions of significantly higher K, such as in the native protein [13,17,19], at low temperature [10,22], at high concentration of TFE [11,12,22] or from idealised values taken from the literature [14–16,18,20,23,24]. Our data thus have implications regarding the quantitative aspects of such analyses, although not necessarily for the qualitative conclusions. Loose structures are probably best described as ensembles of states, in which the tight structure (formed with a numerically larger free energy change than loose structures) will not be highly populated.

Significance

Determination of the stability of secondary structure formation of protein fragments has been used to investigate the probability of the corresponding region of native protein being involved in the initiation of folding. Such experiments have often relied upon knowledge of a measurable parameter relating to the fragment in both its fully folded state and in its fully dissociated state (random coil). This parameter has then been measured for the partially associated system and the population of the associated state has been deduced via a two-state analysis. Our results, which show a significant dependence of the fully associated parameter upon K (the equilibrium constant of the association), imply that such two-state analyses will therefore incorporate an intrinsic error leading to an underestimate of the population of associated states.

Materials and methods

^{1}H NMR spectroscopy

All samples were prepared at pD 3.7 by adjusting the pD of a solution of KD_2PO_4 (50 mM) to approximately pD 3.0 using NaOD and CD_3CO_2D; following addition of the antibiotic (which had been lyophilised twice from D_2O), the pD was adjusted to pD 3.7. All pD measurements were made using a Corning pH meter equipped with a combination glass electrode and no corrections were made for isotope effects. Spectra were recorded at 300K on a Bruker DRX500 spectrometer and calibrated with internal sodium trimethylsilylpropionate (δ = 0 ppm). One-dimensional (1D) spectra were recorded with 16K data points and two-dimensional (2D) spectra were recorded with 2K points in f_2 and 512 increments in f_1. Suppression of solvent was achieved by pre-saturation and time-proportional phase incrementation was used to achieve quadrature detection in the indirect dimension. Data were processed with XWIN-NMR software, with 2D processing employing a sine-squared window function and zero-filling in f_1 up to 1K points.

Determination of monomer and dimer chemical shifts

When monomer and dimer forms of the antibiotic were in fast exchange on the NMR timescale, the chemical shift (δ) of x_4 was typically measured from 1D spectra obtained at a range of concentrations (between 3 mM and 25 or 100 mM, depending on the particular antibiotic). Monomer and dimer chemical shifts were obtained from a plot of δx_4 against antibiotic concentration. Fitting of the curve using a least-squares procedure [25] in Kaleidagraph (Abelbeck Software) and extrapolation to infinitely dilute and infinitely high antibiotic concentrations yielded the required monomer and dimer shifts, respectively. Where peak overlap precluded the observation of x_4 in 1D spectra, it was assigned from 2D NOESY spectra, typically employing a mixing

time of 100 ms. In cases when monomer and dimer were in slow exchange on the NMR timescale, the x_4 signals due to monomer and dimer were correlated by pre-irradiation of the dimer signal, which led to a reduction in the intensity of the monomer signal. For these antibiotics, appearance of the monomer signal could be followed in the 10 μM to 5 mM concentration range.

Determination of dimerisation constants

For antibiotics where the monomer and dimer species were in fast exchange on the NMR timescale, δx_4 was measured as a function of antibiotic concentration [6]. A graph of δx_4 against antibiotic concentration was plotted and the dimerisation constant calculated using a least-squares curve-fitting program [25] in Kaleidagraph. For antibiotics where the monomer and dimer species were in slow exchange on the NMR timescale, at sufficiently low concentrations of antibiotic (10–100 μM), both monomer and dimer states were populated. Integration of corresponding monomer and dimer peaks allowed direct calculation of the dimerisation constant.

Acknowledgements

We are grateful to Eli Lilly (Indianapolis, USA), Abbott Laboratories (Chicago, USA) and SmithKline Beecham (Harlow, UK) for donations of glycopeptide antibiotics and the Biomedical NMR Centre, NIMR, Mill Hill, UK for access to NMR facilities. The EPSRC and Roussel (B.B.), SmithKline Beecham (A.J.M.) and the Ministry of Agriculture, Forestry and Fisheries, Japan (W.T.) are thanked for funding.

References

1. Searle, M.S., Westwell, M.S. & Williams, D.H. (1995). Application of a generalised enthalpy-entropy relationship to binding co-operativity and weak associations in solution. *J. Chem. Soc., Perkin Trans.* **2**, 141-151.
2. Williams, D.H. & Westwell, M.S. (1996). Weak interactions and lessons from crystallization. *Chem. Biol.* **3**, 695-701.
3. Searle, M.S., *et al.*, & Williams, D.H. (1996). Enthalpic (electrostatic) contribution to the chelate effect: a correlation between ligand binding constant and a specific hydrogen bond strength in complexes of glycopeptide antibiotics with cell wall analogues. *J. Chem. Soc., Perkin Trans.* **1**, 2781-2786.
4. Groves, P., Searle, M.S., Westwell, M.S. & Williams, D.H. (1994). Expression of electrostatic binding cooperativity in the recognition of cell-wall peptide analogues by vancomycin group antibiotics. *J. Chem. Soc., Chem. Commun.* 1519-1520.
5. Waltho, J.P. & Williams, D.H. (1989). Aspects of molecular recognition: solvent exclusion and dimerization of the antibiotic ristocetin when bound to a model bacterial cell-wall precursor. *J. Am. Chem. Soc.* **111**, 2475-2480.
6. Gerhard, U., Mackay, J.P., Maplestone, R.A. & Williams, D.H. (1993). The role of the sugar and chlorine substituents in the dimerization of vancomycin antibiotics. *J. Am. Chem. Soc.* **115**, 232-237.
7. Mackay, J.P., Gerhard, U., Beauregard, D.A., Maplestone, R.A. & Williams, D.H. (1994). Dissection of the contributions toward dimerization of glycopeptide antibiotics. *J. Am. Chem. Soc.* **116**, 4573-4580.
8. Wishart, D.S., Sykes, B.D. & Richards, F.M. (1991). Relationship between nuclear magnetic resonance chemical shift and protein secondary structure. *J. Mol. Biol.* **222**, 311-333.
9. Wagner, G., Pardi, A. & Wüthrich, K. (1983). Hydrogen bond length and ^{1}H NMR chemical shifts in proteins. *J. Am. Chem. Soc.* **105**, 5948-5949.
10. Scholtz, J.M., *et al.*, & Bolen, D.W. (1991). Calorimetric determination of the enthalpy change for the α-helix to coil transition of an alanine peptide in water. *Proc. Natl Acad. Sci. USA* **88**, 2854-2858.
11. Marqusee, S., Robbins, V.H. & Baldwin, R.L. (1989). Unusually stable helix formation in short alanine-based peptides. *Proc. Natl Acad. Sci. USA* **86**, 5286-5290.
12. Jasanoff, A. & Fersht, A.R. (1994). Quantitative determination of helical propensities from trifluoroethanol titration curves. *Biochemistry* **33**, 2129-2135.
13. Wang, Y. & Shortle, D. (1997). Residual helical and turn structure in the denatured state of staphylococcal nuclease: analysis of peptide fragments. *Fold. Des.* **2**, 93-100.
14. Peña, M.C., Rico, M., Jiménez, M.A., Herranz, J., Santoro, J. & Nieto, J.L. (1989). Conformational properties of the isolated 1–23 fragment of human hemoglobin α-chain. *Biochim. Biophys. Acta* **957**, 380-389.
15. Ramírez-Alvarado, M., Serrano, L. & Blanco, F.J. (1997). Conformational analysis of peptides corresponding to all the secondary structure elements of protein L B1 domain: secondary structure propensities are not conserved in proteins with the same fold. *Protein Sci.* **6**, 162-174.
16. Rizo, J., Blanco, F.J., Kobe, B., Bruch, M.D. & Gierasch, L.M. (1993). Conformational behavior of *Escherichia coli* Omp A signal peptides in membrane mimetic environments. *Biochemistry* **32**, 4881-4894.
17. Blanco, F.L., Rivas, G. & Serrano, L. (1994). A short linear peptide that folds into a native stable β-hairpin in aqueous solution. *Nat. Struct. Biol.* 1, 584-590.
18. Jiménez, M.A., *et al.*, & Nieto, J.L. (1994). Helix formation by the phospholipase A_2 38–59 fragment: influence of chain shortening and dimerization monitored by NMR chemical shifts. *Biopolymers* **34**, 647-661.
19. Alexandrescu, A.T., Abeygunawardana, C. & Shortle, D. (1994). Structure and dynamics of a denatured 131-residue fragment of staphylococcal nuclease: a heteronuclear NMR study. *Biochemistry* **33**, 1063-1072.
20. Bradley, E.K., Thomason, J.F., Cohen, F.E., Kosen, P.A. & Kuntz, I.D. (1990). Studies of synthetic helical peptides using circular dichroism and nuclear magnetic resonance. *J. Mol. Biol.* **215**, 607-622.
21. Searle, M.S., Williams, D.H. & Packman, L.C. (1995). A short linear peptide derived from the N-terminal sequence of ubiquitin folds into a water-stable non-native β-hairpin. *Nat. Struct. Biol.* **2**, 999-1006.
22. Merutka, G. & Stellwagen, E. (1989). Analysis of peptides for helical prediction. *Biochemistry* **28**, 352-357.
23. Chen, Y.-H., Yang, J.T. & Chau, K.H. (1974). Determination of the helix and β forms of proteins in aqueous solution by circular dichroism. *Biochemistry* **13**, 3350-3359.
24. Greenfield, N. & Fasman, G.D. (1969). Computed circular dichroism spectra for the evaluation of protein conformation. *Biochemistry* **8**, 4108-4116.
25. Press, W.H., Flannery, B.P., Tenkolsky, S.A. & Vetterling, W.T. (1989). *Numerical Recipes in Pascal.* Cambridge University Press, Cambridge, UK.